# Deadtime Correction Method Using Random Coincidence for PET

Seiichi Yamamoto, Masaharu Amano, Shuichi Miura, Hidehiro Iida, and Iwao Kanno

*Department of Engineering for Medical Systems, Shimadzu Corporation, Kyoto; and Division of Radiology and Nuclear Medicine, Research Institute of Brain and Blood Vessels, Akita, Japan*

A deadtime correction method is proposed for quantitative measurements in positron emission tomography. The correction is based on the observation that a deadtime loss of the random coincidence events corresponds to that of the single events and of the total coincidence events. Using the proposed correction method, the deadtime loss was kept within 1% up to the true coincidence rate of $50 \times 10^3$ cps per plane for a cylindrical phantom of 20 cm in diameter. Accuracy of the method is confirmed to be independent of the size of the object.

**J Nucl Med 27:1925–1928, 1986**

A correction for deadtime is indispensable to a quantitative measurement in positron emission tomography (PET) as well as correction for attenuation, detector efficiency, random coincidence, and scattered coincidence. Deadtime causes an underestimation of pixel value of the reconstructed image. This error is sometimes magnified in such physiological models as oxygen-15 ($^{15}O$) gas steady state method (*1*). In the case of dynamic measurement of $^{15}O$ water bolus injection method (*2*), the true coincidence rate increases up to $50 \times 10^3$ cps per plane. Deadtime loss is >20% at this range of true coincidence rate (*3–5*). Several deadtime correction methods have been proposed in recent papers. Mazoyer et al. proposed a scheme which was based on the paralyzing deadtime model using the total coincidence rate (*6*). Hoffman et al. measured the triple coincidence rate to calculate the deadtime loss (*4*). Stearns et al. measured deadtime losses for both single events and total coincidence events independently, then corrected the deadtime (*7*). In some of these methods, accuracy of the correction is often affected by the size of the object.

Figure 1 shows the count rate characteristics of true coincidence for a direct slice of the Headtome III (*3*). These curves were obtained during decay of $^{15}O$ (half-life 123 sec) dissolved in three cylindrical phantoms with different diameters, resulting in different shapes. This means that the true coincidence rate is affected by the size of the object. Therefore, deadtime correction based on a measured true coincidence rate may result in a wide margin of error because one curve cannot be used to correct another.

We have developed a deadtime correction method which is independent of the size of the object. The following is a theoretical analysis and description of some experimental results of this method.

## THEORY

Bismuth germanate (BGO) detectors, timing discriminators, and group encoders work at every single event where rate is proportional to incident annihilation photons. On the other hand, a coincidence logic and a memory work only when a coincidence event occurs. Thus, deadtime losses for single events and that for coincidence events are independent of each other, and should be dealt with independently. As input of the coincidence logic already includes the deadtime loss for single events, the counting efficiency of total coincidence events is a product of a square of the counting efficiency of single events and that of coincidence events. The coincidence logic measures "on-time" events and "off-time" events in the same circuit— the deadtime of "on-time" events and "off-time" events are the same. The total coincidence rate is the sum of the "on-time" rate and the "off-time" rate, i.e., true coincidence rate plus twice of random coincidence rate (*8*). The following relations can be derived from these considerations. When $G_s$ is counting the efficiency of a single rate, the observed single rate after deadtime loss is given by

Received Feb. 27, 1986; revision accepted June 12, 1986.

For reprints contact: Seiichi Yamamoto, Dept. of Engineering for Medical Systems, Shimadzu Corporation, 1, Nishinokyo-Kuwabaracho, Kyoto 604, Japan.

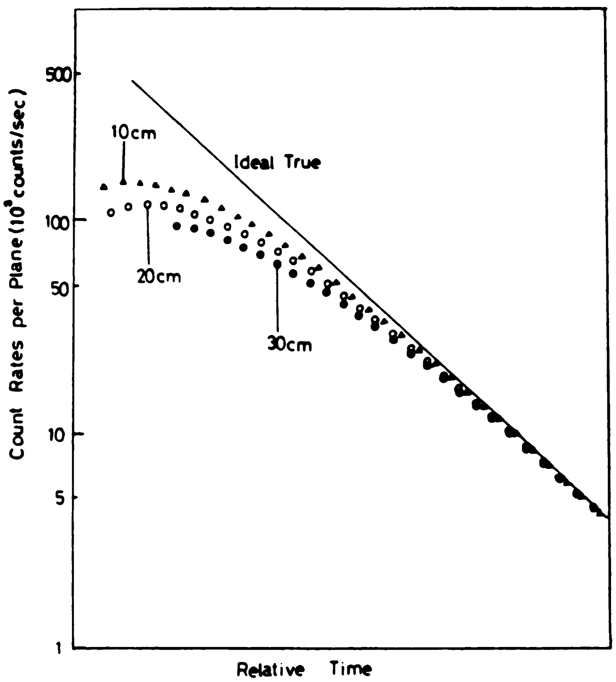


**FIGURE 1**
**Count rate characteristics of true coincidence of the Headtome III for cylindrical phantoms of different diameters**

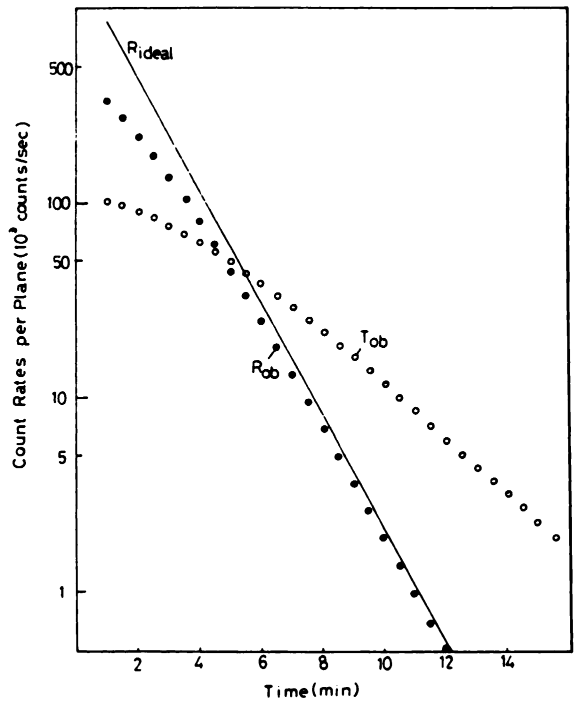


**FIGURE 2**
**Count rate curves of true coincidence rate ($T_{ob}$), random coincidence rate ($R_{ob}$), and calculated ideal random coincidence rate ($R_{ideal}$) for cylindrical phantom of 18 cm in diameter**

$$S_{ob} = G_S \, S_{ideal}, \tag{1}$$

where $S_{ideal}$ is the single rate without deadtime loss. When $G_c$ is counting efficiency for coincidence rate, observed coincidence rate, $C_{ob}$, is given by

$$\begin{aligned} C_{ob} &= G_c \,(\text{"on-time" rate} + \text{"off-time" rate}) \\ &= G_c \,[(T_{ideal}G_s^2 + R_{ideal}\, G_s^2) + R_{ideal}\, G_s^2] \\ &= G_c \, G_s^2 \,(T_{ideal} + 2R_{ideal}), \end{aligned} \tag{2}$$

where $T_{ideal}$ = true coincidence rate without deadtime loss; and

$R_{ideal}$ = random coincidence rate without deadtime loss.

On the other hand, observed random coincidence rate, $R_{ob}$, can be obtained by the "off-time" coincidence,

$$R_{ob} = G_c \, G_s^2 \, R_{ideal}. \tag{3}$$

$R_{ideal}$ can be obtained graphically by extrapolating the measured curve of random coincidence rate. From the count rate curve of random coincidence, we can analytically determine a deadtime correction factor, C, as a function of the observed random coincidence rate,

$$C = 1/(G_c \, G_s^2). \tag{4}$$

The determined correction factor is multiplied to an observed true coincidence rate, $T_{ob}$,

$$T_{ideal} = C \, T_{ob}. \tag{5}$$

## METHODS AND RESULTS

In order to evaluate the accuracy of our proposed method for deadtime correction, phantom experiments were performed. First, the value of the correction factor was determined experimentally. During the decay of $^{15}O$ dissolved in a cylindrical phantom of 18 cm in diameter, $T_{ob}$ and $R_{ob}$ were measured (Fig. 2). $R_{ideal}$ was estimated by an upward extrapolation from the tail of $R_{ob}$. The correction factor is given as a ratio of $R_{ideal}$ to $R_{ob}$. Figure 3 shows a calculated result of the correction factor as a function of the $R_{ob}$. The plotted data in Fig.

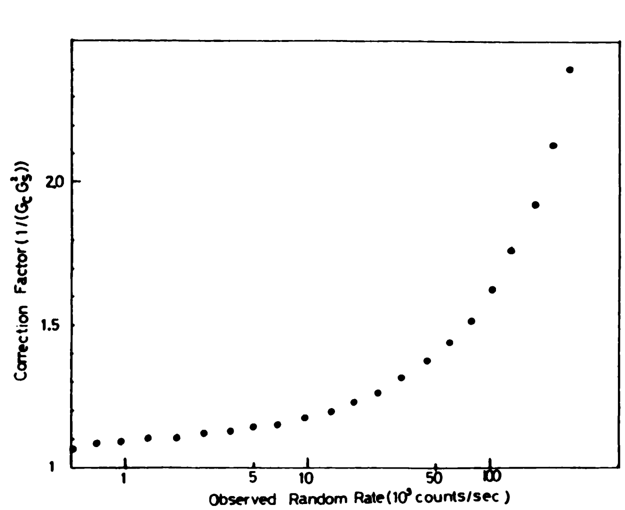


**FIGURE 3**
**Calculated result of correction factor, $1/(G_c\, G_s^2)$, as function of observed random coincidence rate**

3 were fitted by a monotonically increasing function

$$C(R_{ob}) = 1/(1 - \alpha R_{ob}^{\beta/2})^2. \tag{6}$$

The parameters, $\alpha$ and $\beta$, were determined by using a least square fit so as to minimize an error between the observed data and the function. These procedures were applied to each imaging slice including cross slice.

Second, the function was tested using several phantoms. Cylindrical phantoms of different diameters were measured successively during the decay of gallium-68 (half-life 68 min). During the measurements, $R_{ob}$ was monitored by a digital counter and fed to the computer. The correction factor was given using Eq. (6) and $R_{ob}$. The correction factor was multiplied to the pixel value of the image. For each reconstructed image, a region of interest (ROI) was set and average pixel value in the ROI was estimated. The results for three different phantoms for direct slice are shown in Fig. 4. A decay correction was performed simultaneously. A large deadtime loss was observed for the cylindrical phantom of 20 cm in diameter without deadtime correction. Deadtime loss was almost eliminated to <1% up to the true coincidence rate of $50 \times 10^3$ cps per plane with deadtime correction. Without changing any parameters for the deadtime correction, the deadtime losses were also eliminated to <1% up to the true coincidence rate of $60 \times 10^3$ cps and $30 \times 10^3$ cps per plane for 10 cm and 30 cm cylindrical phantoms, respectively. Similar results were obtained in the other imaging slices.

## DISCUSSION AND CONCLUSION

A deadtime correction method which can accurately correct independent of the size of the object was presented. Although the characteristic of deadtime mainly depends on a design of electronic circuits of a PET, the present method can be applied to some other PET systems. In the case of the Headtome III, the deadtime loss at a low count rate is almost determined at the group encoder where sixteen signals are ORed and which has deadtime of 140 ns. On the other hand, at a high count rate, the deadtime loss is determined at both group encoder and coincidence logic which has the deadtime of 150 ns because the random coincidence rate increases proportional to the square of the activity. These conditions of the deadtime loss seem to be the same for most of the PET systems. Therefore, if PET measures the "off-time" coincidence with the same deadtime for "on-time," this deadtime correction method can be applicable according to the authors' experiences.

The observed true coincidence rate ($T_{ob}$) in brain study by the $^{15}O$ gas steady state method was $10 \times 10^3$ cps per plane for direct slice. At this count rate, the correction factor was 1.05. However, in a dynamic measurement of the $^{15}O$ water bolus injection method, the $T_{ob}$ sometimes exceeded $50 \times 10^3$ cps per plane, at which count rate the correction factor was ~1.3. Thus, quantitative measurements cannot be obtained without the deadtime correction. The $T_{ob}$ often exceeded $15 \times 10^3$ cps per plane even in the fluorine-18 fluorodeoxyglucose method, where the deadtime loss reaches ~10%. Further, in the case of heart study which is surrounded by a large object, $T_{ob}$ and $R_{ob}$ were almost $50 \times 10^3$ cps and $100 \times 10^3$ cps per plane, respectively. The correction factor was close to 2.0 in this case.

The most critical studies for deadtime correction are those using $^{15}O$-labeled tracers. Using the Headtome III, routine administration doses of $H_2{}^{15}O$ injection are 25 mCi in the brain study and 15 mCi in the heart study. These doses typically give the true count rates of 35–45 $\times 10^3$ cps and 50–60 $\times 10^3$ cps per plane at peak,

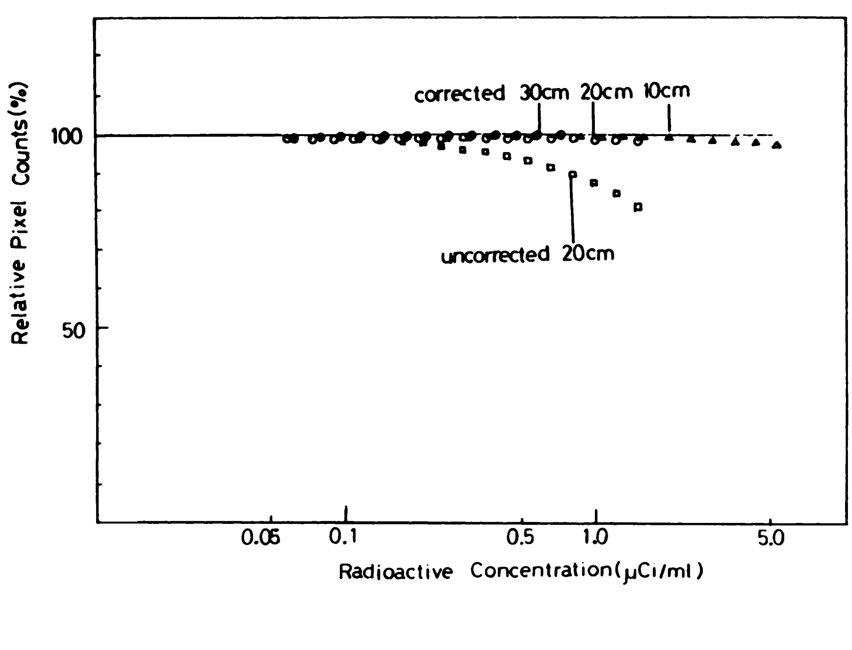


**FIGURE 4**
Relative pixel values in ROI in images of cylindrical phantoms with and without deadtime correction

respectively. Utilizing these count rates, error of the deadtime correction is kept at ~1%. With a higher count rate, for example, using 100 mCi of $^{15}O$ for brain studies, results in the error of deadtime correction becoming >1%. The percentage of error may be kept to a minimum, however, with deadtime correction, while the error might be >100% without the correction. The factor that limits the validity of the deadtime correction is the image distortion due to the multiple events in the group encoders. The count rate that begins to distort the image is the true count rate of around $100 \times 10^3$ cps for 20 cm cylindrical phantom.

## REFERENCES


1. Frackowiak RSJ, Lenzi GL, Jones T, et al: Quantitative measurement of regional cerebral blood flow and oxygen metabolism in man using $^{15}O$ and positron emission tomography: Theory, procedure, and normal values. *J Comput Assist Tomogr* 4:727–736, 1980
2. Raichle ME, Martin WRW, Herscovitch P, et al: Brain blood flow measured with intravenous $H_2{}^{15}O$. II. Implementation and validation. *J Nucl Med* 24:790–798, 1983
3. Kanno I, Miura S, Yamamoto S, et al: Design and evaluation of a positron emission tomograph: Headtome III. *J Comput Assist Tomogr* 9:931–939, 1985
4. Hoffman EJ, Phelps ME, Huang SC: Performance evaluation of positron tomograph designed for brain imaging. *J Nucl Med* 24:245–257, 1983
5. Litton J, Bergstrom M, Eriksson L, et al: Performance study of the PC-384 positron camera system for emission tomograph of the brain. *J Comput Assist Tomogr* 8:74–87, 1984
6. Mazoyer BM, Roos MS, Huesman RH: Deadtime correction and counting statistics for positron tomography. *Phys Med Biol* 30:385–399, 1985
7. Stearns CW, Chesler DA, Kirsch JE, et al: Quantitative imaging with the MGH analog ring positron tomograph. *IEEE Trans Nucl Sci* NS-32:898–901, 1985
8. Derenzo SE, Budinger TF, Huesman RH, et al: Imaging properties of a positron tomograph with 280 BGO crystals. *IEEE Trans Nucl Sci* NS-28:81–89, 1981